



Published in final edited form as:

*Nat Med.* 2016 July ; 22(7): 800–806. doi:10.1038/nm.4101.

## Central injection of fibroblast growth factor 1 induces sustained remission of diabetic hyperglycemia in rodents

Jarrad M. Scarlett<sup>1,2,10</sup>, Jennifer M. Rojas<sup>1,10</sup>, Miles E. Matsen<sup>1</sup>, Karl J. Kaiyala<sup>3</sup>, Darko Stefanovski<sup>4</sup>, Richard N. Bergman<sup>5</sup>, Hong T. Nguyen<sup>1</sup>, Mauricio D. Dorfman<sup>1</sup>, Louise Lantier<sup>6</sup>, David H. Wasserman<sup>6</sup>, Zaman Mirzadeh<sup>7</sup>, Terry G. Unterman<sup>8,9</sup>, Gregory J. Morton<sup>1</sup>, and Michael W. Schwartz<sup>1</sup>

<sup>1</sup>Diabetes and Obesity Center of Excellence, Department of Medicine, University of Washington, Seattle, Washington, USA

<sup>2</sup>Department of Pediatric Gastroenterology and Hepatology, Seattle Children's Hospital, Seattle, Washington, USA

<sup>3</sup>Department of Oral Health Sciences, School of Dentistry, University of Washington, Seattle, Washington, USA

<sup>4</sup>New Bolton Center, School of Veterinary Medicine, University of Pennsylvania, Philadelphia, Pennsylvania, USA

<sup>5</sup>Diabetes and Obesity Research Institute, Cedars-Sinai Medical Center, Los Angeles, California, USA

<sup>6</sup>Department of Molecular Physiology and Biophysics, Vanderbilt School of Medicine, Nashville, Tennessee, USA

<sup>7</sup>Barrow Neurological Institute, St. Joseph's Hospital and Medical Center, Phoenix, Arizona, USA

<sup>8</sup>Section of Endocrinology, Diabetes and Metabolism, Department of Medicine, University of Illinois at Chicago College of Medicine, Chicago, Illinois, USA

<sup>9</sup>Medical Service, Jesse Brown VA Medical Center, Chicago, Illinois, USA

### Abstract

Type 2 diabetes (T2D) is among the most common and costly disorders worldwide<sup>1</sup>. The goal of current medical management of T2D is to transiently ameliorate hyperglycemia through daily

Users may view, print, copy, and download text and data-mine the content in such documents, for the purposes of academic research, subject always to the full Conditions of use: [http://www.nature.com/authors/editorial\\_policies/license.html#terms](http://www.nature.com/authors/editorial_policies/license.html#terms) Reprints and permissions information is available at [www.nature.com/reprints](http://www.nature.com/reprints)

Correspondence should be addressed to M.W.S. ([mschwart@u.washington.edu](mailto:mschwart@u.washington.edu)).

<sup>10</sup>These authors contributed equally to this work.

#### Competing financial interests

The authors declare no competing financial interests.

#### AUTHOR CONTRIBUTIONS

J.M.S., J.M.R., L.L., D.H.W., G.J.M. and M.W.S., designed, funded and supervised the research. J.M.S., J.M.R., M.D.D., Z.M., and M.E.M. performed the research. T.G.U. generated LIRFKO mice. J.M.S., J.M.R., K.J.K., D.S., M.D.D., Z.M., H.T.N., R.N.B., L.L., D.H.W., G.J.M., and M.W.S. analyzed the data. J.M.S., J.M.R., and M.W.S. wrote the manuscript. M.W.S. has final responsibility for the hypothesis, study design, data analysis, interpretation and conclusions, and final approval of the manuscript.

dosing of one or more anti-diabetic drugs. Hypoglycemia and weight are common side effects of therapy, and sustained disease remission is not obtainable with non-surgical approaches. Based on the potent glucose-lowering response elicited by activation of brain fibroblast growth factor (FGF) receptors<sup>2-4</sup>, we explored the anti-diabetic efficacy of centrally administered FGF1, which, unlike other FGF peptides, activates all FGF receptor subtypes<sup>5</sup>. We report that a single intracerebroventricular (i.c.v.) injection of FGF1 at a dose one-tenth of that needed for systemic anti-diabetic efficacy induces sustained diabetes remission in both mouse and rat models of T2D. This anti-diabetic effect is not secondary to weight loss, does not increase the risk of hypoglycemia, and involves a novel and incompletely understood mechanism for increasing glucose clearance from the bloodstream. We conclude that the brain has the inherent potential to induce diabetes remission and that brain FGF receptors are potential pharmacological targets for achieving this goal.

## Keywords

diabetes; fibroblast growth factor; brain

---

Growing evidence points to the brain as a potential target for the treatment of T2D<sup>6,7</sup>. In rodent models of T2D, hyperglycemia can be ameliorated transiently by either systemic or i.c.v. administration of FGF19<sup>2-4,8</sup> or FGF21<sup>9</sup>. Unlike these peptide hormones, which bind to and activate a limited subset of FGF receptors (FGFR) via an interaction that requires the co-receptor  $\beta$ -Klotho, the tissue growth factor FGF1 binds to and activates all known FGFR isoforms without the need for  $\beta$ -Klotho<sup>5</sup>. Moreover, glucose lowering elicited by systemic administration of FGF1 is of longer duration (up to 42 h)<sup>10</sup> than is elicited by either FGF19<sup>2</sup> or FGF21<sup>9</sup>. In the brain, FGF1 is synthesized by neurons, astrocytes, and ependymal cells<sup>11,12</sup>, and central FGF1 administration can enhance learning and memory<sup>12</sup>, reduce food intake<sup>13</sup>, and limit damage associated with ischemic stroke or neurodegenerative disease<sup>14,15</sup>. In addition, a physiological role for FGF1 in glucose homeostasis is implied by the development of diabetes in mice lacking FGF1 challenged with a high fat diet<sup>16</sup>.

We therefore hypothesized that like FGF19 and FGF21, FGF1 action in the brain promotes glucose lowering in rodent models of T2D and, based on its relatively prolonged anti-diabetic action following systemic administration, that glucose lowering induced by i.c.v. FGF1 administration would be long-lived relative to other FGF peptides. To test this hypothesis, we monitored blood glucose levels following a single injection of recombinant mouse FGF1 (mFGF1) into the lateral ventricle of diabetic *ob/ob* mice at a dose (3  $\mu$ g) one-tenth that needed for systemic anti-diabetic efficacy<sup>10</sup>. As predicted, we observed a ~25% decline of fasting blood glucose levels 6 h after i.c.v. injection of mFGF1 (Fig. 1a). Although modest, this effect cannot be explained by either reduced food intake (since food was not available during this time) or by leakage from the brain to the periphery, since subcutaneous (s.c.) administration of the same dose of FGF1 was without effect (Fig. 1b).

To assess the duration of this glucose-lowering effect, we monitored both fasting and *ad-libitum* (*ad-lib*) fed blood glucose levels over time following a single i.c.v. injection of mFGF1. We found that blood glucose levels were fully normalized 7 d later (Fig. 1c,d) and

remained within the normal range (<200 mg/dL) for the next 17 weeks (having concluded that sustained diabetes remission had been achieved, the study was terminated after a total duration of 18 weeks) (Fig. 1c,d). This sustained glucose-lowering effect of i.c.v. FGF1 was not associated with changes of either plasma insulin or glucagon levels (Supplementary Fig. 1a).

Although food intake and body weight were also reduced by i.c.v. mFGF1 in these mice, the effect was transient such that the pronounced improvement of glycemia persisted for months after food intake, body weight and fat mass had returned to normal (Fig. 1e). This finding suggests, but does not establish, that diabetes remission induced by central FGF1 injection is weight loss-independent. To more directly test this hypothesis, two additional groups of *ob/ob* mice were monitored after receiving a single i.c.v. injection of saline vehicle (Veh). One of these groups was allowed to feed *ad-lib* while the other was pair-fed to the amount of food consumed by *ob/ob* mice receiving i.c.v. FGF1. Although blood glucose values declined in the pair-fed group relative to *ad-lib*-fed animals, the effect was both modest and transient and did not reach statistical significance (Fig. 1f). Therefore, sustained diabetes remission induced by the central action of FGF1 cannot be explained by reduced food intake or body weight.

To assess the reproducibility of these findings, we subjected three additional groups of diabetic *ob/ob* mice to a single i.c.v. injection of Veh, recombinant human FGF1 (hFGF1), or mFGF1. Although the onset of glucose lowering in response to hFGF1 was delayed by 24 h, sustained diabetes remission was nevertheless observed following a single i.c.v. injection of either peptide (Fig. 2a). In addition, prolonged glucose lowering accompanied by a transient reduction of food intake and body weight was observed irrespective of whether mFGF1 (3 µg) was injected into the lateral (Fig. 1d,e) or the 3<sup>rd</sup> ventricle (Supplementary Fig. 1b). Hypoglycemia was not elicited by i.c.v. FGF1 in either *ob/ob* mice (Fig. 2a) or in lean, wild-type (WT) controls, whether fed standard chow (Fig. 2b) or a high-fat diet (HFD) (Fig. 2c). Although this ability to ameliorate hyperglycemia without risk of hypoglycemia is shared by both systemic administration of a ~10 fold higher dose of mFGF1 (0.5 mg/kg body weight s.c.; Fig. 2d) and central administration of the same dose of FGF19 (3 µg i.c.v.; Fig. 2e), neither intervention elicits persistent glucose lowering. Sustained diabetes remission induced by the central action of FGF1, therefore, involves mechanisms distinct from those engaged by either systemic FGF1 or i.c.v. FGF19 when administered at doses with comparable short-term glucose-lowering efficacy.

Based on evidence that i.c.v. FGF1 reduces blood glucose levels and suppresses the hypothalamic-pituitary-axis (HPA) in rats with severe diabetic ketoacidosis<sup>17</sup>, we measured plasma corticosterone levels at a fixed time of day (in mid-light cycle, between 1400–1600 h, following a 6 h fast), 6 h after administration of either FGF1 (3 µg) or Veh, into either the lateral ventricle or the 3<sup>rd</sup> ventricle of *ob/ob* mice. Plasma corticosterone levels were not reduced by FGF1 (irrespective of the route of i.c.v. delivery; Supplementary Fig. 2a,b) in these mice, nor was such an effect observed in *ob/ob* mice with sustained FGF1-induced diabetes remission (again, measured during mid-light cycle following a 6 h fast), despite their much lower blood glucose levels (Supplementary Fig. 2c). Diabetes remission induced by i.c.v. FGF1, therefore, cannot be attributed to HPA axis suppression.

To investigate whether sustained diabetes remission induced by centrally administered FGF1 in *ob/ob* mice occurs in other mouse models of T2D, we repeated the experiment in both *db/db* mice (Fig. 2f). We also employed the combination of diet-induced obesity (DIO) with a low dose of the  $\beta$ -cell toxin streptozotocin (DIO-LD STZ) in wild-type mice to model the combination of insulin resistance and beta cell dysfunction of human T2D (Fig. 2g). Our finding that sustained glucose lowering was induced by i.c.v. mFGF1 in each of these mouse models demonstrates that remission of T2D induced by the central action of FGF1 is not limited to *ob/ob* mice. As expected, both food intake and body weight were also reduced following i.c.v. FGF1 in these mouse models (Supplementary Fig. 3a,b), but as in *ob/ob* mice (Supplementary Fig. 3c), these effects were transient such that pronounced glucose lowering persisted well after body weight had returned to control values (Fig. 2f,g).

To determine if FGF1-induced diabetes remission is achievable in a different species, we administered either the same dose (3  $\mu$ g i.c.v.) of recombinant rat FGF1 (rFGF1) or Veh to adult male Zucker Diabetic Fatty (ZDF) rats. Consistent with our findings in mice, diabetes remission lasting >4 weeks was induced by a single i.c.v. injection of rFGF1 in these animals and once again, hypoglycemia was not observed (Fig. 2h), although food intake and body weight were reduced, as expected (Supplementary Fig. 3d). Since pronounced glucose lowering in ZDF rats persisted well after food intake, body weight, and fat mass had returned to control values (Fig. 2h and Supplementary Fig. 3d), we conclude that as in diabetic mice, i.c.v. FGF1 induces weight loss-independent diabetes remission in a rat model of T2D.

To investigate the peripheral mechanisms underlying diabetes remission induced by i.c.v. FGF1, we first measured the rate of plasma glucose clearance in the basal state. We found that despite a ~39% reduction of fasting blood glucose values 1 week following i.c.v. injection of FGF1 (3  $\mu$ g) in *ob/ob* mice (Fig. 3a), there was no difference in the basal glucose turnover rate (GTR; which at steady-state equals the rates of both glucose production and glucose disposal) (Fig. 3b). Implied in this observation is an increased peripheral glucose clearance rate (a measure of the efficiency of glucose removal from the circulation),<sup>18</sup> since the rate of glucose disposal increases as a function of its plasma level. Accordingly, the basal glucose clearance rate was increased two-fold in mice receiving i.c.v. mFGF1 compared to vehicle (Fig. 3b).

To determine whether this increase of basal glucose clearance resulted from an increase of insulin sensitivity (measured as the insulin sensitivity index,  $S_I$ ), insulin secretion (measured as the acute insulin response to glucose,  $AIR_g$ ) or insulin-independent glucose disposal (measured as glucose effectiveness,  $S_g$ ), we performed a frequently sampled intravenous glucose tolerance test (FSIGT) followed by minimal model analysis of blood glucose and plasma insulin data (a method validated in humans,<sup>19</sup> primates,<sup>20</sup> dogs<sup>21</sup> and rodents<sup>2,22,23</sup>) in the same cohort of *ob/ob* mice (Fig. 3a). Although a trend towards improved glucose tolerance was observed in mice receiving prior i.c.v. mFGF1 injection, the effect was not statistically significant after correcting for the difference in basal glucose levels (AUC; Fig. 3a). A tendency for increased glucose-induced insulin secretion ( $AIR_g$ ) was also observed in the group receiving i.c.v. FGF1, but this effect did not achieve statistical significance, nor did increases of either  $S_I$  or  $S_g$  (Fig. 3a,c). Sustained diabetes remission induced by the

central action of FGF1, therefore, involves a novel mechanism characterized by increased peripheral glucose clearance in the basal state with no change of basal hepatic glucose production, glucose tolerance, or in any of the three determinants of glucose tolerance ( $S_I$ ,  $AIR_g$ , and  $S_g$ ).

Relative to i.c.v. Veh-treated controls, both hepatic glycogen content and hepatic expression of genes encoding the key glucoregulatory enzymes glucokinase (*Gck*), liver-type pyruvate kinase (*Pklr*) and glycogen synthase (*Gys2*) were increased in *ob/ob* mice 1 week following i.c.v. mFGF1 (Fig. 3d). Combined with an increase of basal plasma lactate levels (Fig. 3d) that is suggestive of increased intrahepatic glycolysis<sup>2,24,25</sup>, diabetes remission induced by i.c.v. FGF1 appears to involve increased hepatic glucose uptake (HGU) with subsequent increases of both glycogen synthesis and glycolysis. In contrast, the expression of hepatic gluconeogenic genes phosphoenolpyruvate carboxykinase (*Pck1*) and glucose-6-phosphatase (*G6pc*) were not altered by i.c.v. mFGF1 (Fig. 3d), consistent with the absence of any effect on basal GTR.

To determine if tissues other than the liver contribute to the FGF1-mediated increase of basal glucose clearance, we collected tissues from *ob/ob* mice following continuous intravenous (i.v.) infusion of radiolabeled 2-deoxyglucose 1 week after a single i.c.v. injection of mFGF1 (3  $\mu$ g) or Veh. Mixed model analysis revealed that the rate of glucose clearance (Kg) into skeletal muscle, but not heart, adipose tissue or brain, was increased following i.c.v. FGF1 (after adjusting for the four skeletal muscle types sampled; see Methods) (Fig. 3e). Thus, diabetes remission induced by i.c.v. FGF1 appears to involve increases of basal glucose clearance into both liver and skeletal muscle, but not other tissues. Combined with the lack of any change of uncoupling protein-1 (*Ucp1*) gene expression in brown adipose tissue (BAT) from *ob/ob* mice receiving i.c.v. mFGF1 (Supplementary Fig. 4a), these observations indicate that BAT thermogenesis is unlikely to contribute to diabetes remission induced by i.c.v. FGF1. Similarly, diabetes remission induced by i.c.v. FGF1 administration was not associated with reduced plasma levels of triglycerides, cholesterol, or non-esterified free fatty acids (NEFA) in either *ob/ob* or *db/db* mice (Supplementary Fig. 4b,c).

Unlike the lack of glycemic regulation characteristic of uncontrolled type 1 diabetes<sup>26</sup>, the pathogenesis of T2D appears to involve regulation of glycemia at an elevated level<sup>27</sup>. This distinction provides a useful context within which to consider our finding that although i.c.v. FGF1 worked well in both mouse and rat models of T2D with moderate hyperglycemia, it was ineffective in mice with more severe, uncontrolled hyperglycemia (blood glucose >300 mg/dl). This observation applies not only to *db/db* mice and DIO WT mice receiving a high dose of STZ (Supplementary Fig. 5a,b), but also to *ob/ob* mice crossed onto the diabetogenic BTBR background (Supplementary Fig. 5c).

One potential explanation for this outcome is that FGF1-mediated glucose lowering requires an intact insulin signal; i.e., that intact basal insulin action is permissive for diabetes remission induced by central FGF1. To formally test this hypothesis, we administered the high-affinity insulin receptor (IR) antagonist S961<sup>28</sup> to DIO WT mice as a continuous s.c. infusion at a dose (29 nmol/week) designed to achieve the moderately elevated blood glucose levels characteristic of FGF1-responsive *ob/ob* mice (on the C57B16J background;

Fig. 1d). Although we observed the expected, transient reduction of food intake and body weight following i.c.v. mFGF1 in S961-treated mice (Supplementary Fig. 5d), glucose lowering did not occur (Supplementary Fig. 5d). Thus, intact insulin signaling appears to be required for diabetes remission induced by the central action of FGF1.

In hepatocytes, the glucose-lowering action of insulin depends on inactivation of the transcription factor FoxO1<sup>29</sup>, and in mice with deficient hepatic insulin signaling, increased FoxO1 signaling potently inhibits HGU<sup>30,31</sup>. These observations raise the possibility that activation of hepatic FoxO1 induced by insulin receptor blockade underlies the observed resistance to FGF1-mediated glucose lowering. To test this hypothesis, we studied the effect of i.c.v. mFGF1 in mice with liver-specific deletion of both FoxO1 and insulin receptor (liver IR/FoxO1 double knockout, or LIRFKO, mice<sup>30</sup>) in which hyperglycemia was induced by systemic S961 administration. As expected, insulin receptor blockade induced by S961 did not impair the ability of i.c.v. FGF1 to reduce food intake and body weight (Supplementary Fig. 6a,b), but hyperglycemia elicited by systemic IR blockade was not ameliorated by centrally administration of FGF1 in either LIRFKO mice or their controls (Supplementary Fig. 6a,b). Resistance to FGF1-mediated glucose lowering conferred by IR blockade therefore involves mechanisms additional to hepatic FoxO1 activation.

As cells responsive to both glucose and FGF1<sup>32,33</sup>, tanycytes lining the 3<sup>rd</sup> ventricle adjacent to the mediobasal hypothalamus have interesting potential as mediators of FGF1-induced diabetes remission. To determine if the response of these cells to FGF1 (which induces sustained diabetes remission) differs from that elicited by FGF19 (which does not induce diabetes remission), we used immunohistochemistry to detect c-Fos, a marker of cellular activation, 90 min following injection into the lateral ventricle of Veh, FGF1 or FGF19. Whereas i.c.v. FGF1 induced robust c-Fos expression in 3<sup>rd</sup> ventricular tanycytes, FGF19 did not (Supplementary Fig. 7a,b), raising the possibility of a functional link between activation of 3<sup>rd</sup> ventricular tanycytes and diabetes remission induced by FGF1.

Hypothalamic expression of heat-shock protein 25 (the mouse homologue of human HSP27), a potent neuroprotectant molecule<sup>34</sup>, is highly responsive to FGF1 stimulation. Confirming a previous report<sup>13</sup>, we observed a marked increase of hypothalamic HSP25 (*Hspb1*) mRNA 6 h following i.c.v. injection of mFGF1 (3 µg) in non-diabetic control mice (Supplementary Fig. 7c). To determine if 3<sup>rd</sup> ventricular tanycytes are among the cells in which HSP25 is induced by FGF1, we employed whole-mount immunostaining of the 3<sup>rd</sup> ventricular wall to detect expression of HSP25 24 h after a single i.c.v. injection of either mFGF1 or Veh. Coupled with confocal microscopy, this method provides an en-face perspective not only of ependyma and tanycytes lining the ventricular surface, but also of neurons and glia in hypothalamic parenchyma at a depth of up to 80 µm<sup>35</sup>. We found that i.c.v. FGF1 induced robust expression of HSP25 in both a discrete band of tanycytes (Fig. 4a–c) in the posterior ventral aspect of the 3<sup>rd</sup> ventricular surface and in subependymal, stellate-shaped astrocytes (Fig. 4d) adjacent to the 3<sup>rd</sup> ventricle. In contrast, neuronal expression of HSP25 was not detected, nor was this protein detected in tanycytes or astrocytes in mice receiving i.c.v. Veh (Fig. 4e–g).

To investigate whether i.c.v. FGF1 affects hypothalamic synaptic content, we quantified the level of synaptophysin<sup>36,37</sup>, a synaptic marker, in hypothalamic extracts obtained 1 week following a single i.c.v. injection of mFGF1 or Veh in *ob/ob* mice. Our finding of a 24% increase of hypothalamic synaptophysin content in FGF1-treated mice is suggestive of increased synaptic density in this brain area (Supplementary Fig. 7d).

Beyond certain bariatric surgical procedures, we are unaware of any intervention capable of inducing remission of T2D in humans or rodents. Here, we report that in multiple rodent models of T2D, a single i.c.v. dose of FGF1 restores blood glucose levels to the normal range in a manner that is sustained for weeks, is not associated with hypoglycemia, is not secondary to changes of energy balance or fat stores, and is apparently mediated by increased glucose clearance into both liver and skeletal muscle.

The liver's enormous capacity for glucose uptake contributes substantially to glucose clearance following a meal<sup>38</sup>. Although rising concentrations of glucose in the hepatic portal vein are the primary stimulus driving increased HGU, signals emanating from the brain are also implicated<sup>38</sup>. In light of our evidence linking increased HGU to FGF1-mediated glucose lowering, we speculate that diabetes remission induced by i.c.v. FGF1 involves an action on neurocircuits that normally serve to enhance HGU following a meal. Increased glucose clearance into skeletal muscle also appears to contribute to FGF1-mediated diabetes remission, and each of these effects occurred in the absence of increases of either basal insulin levels or glucose-induced insulin secretion. Since measures of insulin secretion were made at a time when blood glucose levels were lower in FGF1- than in Veh-treated mice, however, it remains possible that an effect of central FGF1 to enhance insulin secretion was masked by the concurrent decrease of blood glucose levels. Combined with our finding that systemic insulin receptor blockade disrupts FGF1-mediated glucose lowering, additional study of insulin's role in FGF1-mediated diabetes remission is needed.

Although systemic FGF1 administration also has anti-diabetic effects, it does not induce sustained diabetes remission<sup>10</sup>. This observation implies that the central nervous system (CNS) mechanisms activated by administration of FGF1 directly into the brain are not engaged by circulating FGF1. This possibility is strengthened by evidence that glucose lowering induced by systemic FGF1 requires FGFR1 signaling in adipose tissue<sup>10</sup>, a mechanism unlikely to explain the action of FGF1 in the brain.

A physiological role for hypothalamic FGF1 signaling in metabolic homeostasis was first suggested by evidence that FGF1 expressed in cells lining the 3<sup>rd</sup> cerebral ventricle, adjacent to the mediobasal hypothalamus (MBH), is released locally following a meal<sup>12</sup>. Tanycytes (rather than ependymal cells) are the predominant cell type lining the 3<sup>rd</sup> ventricle in the area of the MBH<sup>35</sup>. These cells have interesting potential as candidate mediators of FGF1 action, since they send long, filamentous projections from the ventricular surface into adjacent hypothalamic parenchyma that can influence neuronal function, are responsive both to glucose<sup>39,40</sup> and FGFs<sup>33</sup>, and are implicated as a source of hypothalamic neural progenitor cells<sup>33</sup>. In this context, our finding that 3<sup>rd</sup> ventricular tanycytes are robustly activated by i.c.v. FGF1 (based on induction of c-Fos, a marker of cellular activation), but not by i.c.v. FGF19, is of interest given that glucose lowering by i.c.v. FGF1 is sustained,

whereas that induced by i.c.v. FGF19 is not. Thus, the activation of these cells by FGF1 tracks with the ability of FGF peptides to induce diabetes remission. We further demonstrate that in response to i.c.v. FGF1, the potent neuroprotective protein HSP25 is induced in both 3<sup>rd</sup> ventricular tanycytes and an adjacent set of periventricular astrocytes<sup>13</sup>, but not in hypothalamic neurons. These observations justify additional investigation into the role of tanycytes in FGF1-mediated diabetes remission.

A remarkable aspect of glucose lowering induced by i.c.v. FGF1 is that it occurs only in hyperglycemic and not in non-diabetic animals. To account both for this selectivity and for the sustained nature of its anti-diabetic effect, we hypothesize that 1) neurocircuits involved in glucose homeostasis are dysfunctional in T2D, 2) this dysfunction contributes to hyperglycemia, and 3) FGF1 ameliorates this dysfunction without impacting the same neurocircuits in non-diabetic animals. Accordingly, one might anticipate that in diabetic mice, central FGF1 administration elicits structural changes in brain areas involved in glucoregulation. Although preliminary, our finding of an association between FGF1-induced diabetes remission and a modest increase in whole hypothalamic content of synaptophysin, a synaptic marker protein<sup>36,37</sup>, implies that either synaptogenesis was increased or that synaptic pruning was decreased (or both). Additional studies to address these possibilities and to identify the hypothalamic areas involved are warranted.

In conclusion, we report that central FGF1 administration unmasks the brain's inherent capacity to induce sustained diabetes remission. This effect is elicited without the risk of hypoglycemia, in a manner that is truly weight loss-independent, via a novel peripheral mechanism characterized by increased glucose clearance into skeletal muscle and liver, and without the need for surgical revision of the gastrointestinal tract. The translational relevance of this discovery is heightened by the feasibility of therapeutic FGF1 delivery to the CNS via the intranasal route, which has been established in rodents<sup>14,21</sup>. Translational studies are warranted to determine if this type of strategy may one day be employed to promote diabetes remission in humans.

## ONLINE METHODS

### Animals

Male, 8-week-old *ob/ob* (B6.Cg-Lep<sup>ob</sup>/J), *ob/ob* (BTBR.Cg-Lep<sup>ob</sup>/WiscJ), *db/db* (B6.BKS(D)-Lepr<sup>db</sup>/J), and C57BL/6J (WT) mice were purchased from Jackson Laboratories (Bar Harbor, ME). Transgenic FGFR1-EGFP (GP338Gsat/Mmucd) mice were obtained from the Mutant Mouse Regional Resource Center (UC Davis, Davis, CA) and analysis was performed on male, 8-week-old mice. Male, 5-week-old ZDF rats (ZDF-Lepr<sup>fa</sup>/Crl) were purchased from Charles River and analysis was performed on 8-week-old rats. To generate male, 8-week-old liver-specific double knockout of the IR and FoxO1 (LIRFKO) mice and littermate controls (IRF fl/fl), we crossed IR(fl/fl); FoxO1(fl/fl); Albumin-Cre(tg/wt) mice to IR(fl/fl); FoxO1(fl/fl); Albumin-Cre(wt/wt) animals on a mixed (C57BL6/J-FVB/N) background, as previously described<sup>30</sup>. All animals were housed individually under specific pathogen-free conditions in a temperature-controlled room with a 12:12 h light:dark cycle. Mice were provided with *ad-libitum* (*ad-lib*) access to water and either standard laboratory chow (LabDiet, St. Louis, MO) or a 60% high-fat diet (HFD;

D12492, Research Diets, New Brunswick, NJ), unless otherwise stated. ZDF rats were provided with *ad-lib* access to water and Purina 5008 diet (Animal Specialties, Inc., Hubbard, OR). All procedures were performed in accordance with NIH guidelines for the care and use of animals and were approved by the Institutional Animal Care and Use Committee at either the University of Washington (Seattle, Washington) or Vanderbilt University (Nashville, Tennessee). Except as noted below, we did not exclude any animals from analysis. Mice and rats were randomly assigned into various surgical and treatment groups detailed below with no blinding.

### Criteria for sustained diabetes remission

Based on evidence that in non-diabetic, wild-type mice, blood glucose levels obtained under *ad-lib* fed conditions are typically in the range of 100 mg/dl and rarely exceed values of 150 mg/dl (Fig. 2b and unpublished data), sustained remission of diabetes was defined as a reduction of mean blood glucose levels obtained under *ad-lib* fed conditions to values <200 mg/dl that lasted for at least 4 weeks. Studies investigating whether sustained diabetes remission occurred were therefore conducted for a minimum of 4 weeks, with blood glucose levels obtained under *ad-lib* fed conditions at least once per week. To assess the durability of diabetes remission induced by i.c.v. FGF1, some studies were conducted for up to 18 weeks. Animals meeting the above criteria for >4 mo were deemed to have stable and seemingly permanent diabetes remission.

### Surgery

Cannulation of the third ventricle (3<sup>rd</sup> V) or lateral ventricle (LV; 26-ga, Plastics One, Roanoke, VA) were performed under isoflurane anesthesia using the following stereotaxic coordinates:<sup>41,42</sup> For mice, 3<sup>rd</sup> V: -1.8 mm posterior to bregma; mid-line, and -4.3 mm below the skull surface; LV: -0.7 mm posterior to bregma; 1.3 mm lateral, and 1.3 mm below the skull surface; and for rats, LV: -0.8 mm posterior to bregma; 1.5 mm lateral, and 2.6 mm below the skull surface. For measurement of basal glucose turnover followed by a FSIGT, adult male *ob/ob* (B6) mice underwent LV cannulation and catheterization of both the carotid artery and the internal jugular vein during the same surgical session. Animals received buprenorphine hydrochloride (Reckitt Benckiser Pharmaceuticals Inc., Richmond, VA) at the completion of the surgery and were allowed to recover for at least 7 d prior to study while food intake and body weight were recorded. We excluded from the study mice and rats whose body weight had not recovered 7 d after surgery.

### Intracerebroventricular (i.c.v.) injections

Rodents were monitored for several days to ensure that mean blood glucose values were matched between study groups prior to i.c.v. injection. For i.c.v. injections via the 3<sup>rd</sup> V in mice, recombinant mouse FGF1 (mFGF1; Prospec-Tany TechnoGene Ltd, East Brunswick, NJ) was dissolved in sterile water at a concentration of 3 µg/µl and injected over 60 s in a final volume of 1 µl using a (33-ga) needle extending 1 mm beyond the tip of the i.c.v. cannula. For i.c.v. injections via the LV in mice, recombinant mouse FGF1 (mFGF1; Prospec-Tany TechnoGene Ltd, East Brunswick, NJ) or recombinant human FGF1 (hFGF1; a generous gift from Novo Nordisk) were dissolved in sterile water or phosphate-buffered saline (PBS), respectively, at a concentration of 1.5 µg/µl and injected over 60 s in a final

volume of 2  $\mu\text{l}$  using a (33-ga) needle extending 0.8 mm beyond the tip of the i.c.v. cannula. Recombinant human FGF19 (Phoenix Pharmaceuticals, Burlingame, CA) was dissolved in 0.9% normal saline at a concentration of 2  $\mu\text{g}/\mu\text{l}$  and was administered via the LV as previously described<sup>2</sup>. Recombinant rat FGF1 (rFGF1; Prospec-Tany TechnoGene Ltd, East Brunswick, NJ) was dissolved in sterile water at a concentration of 1  $\mu\text{g}/\mu\text{l}$  and injected over 60s into the LV in a final volume of 3  $\mu\text{l}$  using a (33-ga) needle extending 1 mm beyond the tip of the i.c.v. cannula.

### Intraperitoneal glucose tolerance testing

ipGTTs were conducted in 6 h-fasted animals by measuring blood glucose levels at  $t = 0, 15, 30, 60, 90,$  and 120 min from a tail capillary blood sample using a hand-held glucometer (Abbott FreeStyle Lite, Abbot Diabetes Care, Alameda, CA) following an intraperitoneal (i.p.) injection of glucose (30% dextrose) at a dose of either 0.5 or 2 g/kg body weight, depending on basal glycemia.

### Body composition analysis

Total body fat mass was measured using quantitative magnetic resonance spectroscopy (EchoMRI 3-in-1 Animal Tissue Composition Analyzer; Echo Medical Systems, Houston, TX) available through the Energy Balance and Glucose Metabolism Core of the NIDDK-funded Nutrition Obesity Research Center at the University of Washington.

### Subcutaneous injections

Recombinant mouse FGF1 (mFGF1; Prospec-Tany TechnoGene Ltd, East Brunswick, NJ) was dissolved in sterile water at a concentration of 1.5  $\mu\text{g}/\mu\text{l}$  and administered s.c. in a final volume of 50  $\mu\text{l}$  of vehicle (Veh) solution (0.9% normal saline).

### DIO WT-STZ mice

After consuming a HFD for 3 mo to induce diet-induced obesity (DIO), WT mice underwent cannulation of the LV and 7 d later received either three consecutive daily i.p. injections of streptozotocin (STZ; Sigma-Aldrich, St. Louis, MO) at a low dose (40 mg/kg body weight) (DIO-LD STZ) to induce moderate hyperglycemia (~150–200 mg/dl), or a single s.c. injection of a high dose of STZ (100 mg/kg body weight) to induce more severe hyperglycemia (DIO-HD STZ). Measures of blood glucose blood glucose levels, food intake, and body weight were recorded throughout the study.

### Basal glucose turnover

Basal glucose turnover analysis (as previously described<sup>43</sup>) was performed in 5 h-fasted *ob/ob* (B6) mice 7 d after receiving i.c.v. injection of either mFGF1 (3  $\mu\text{g}$ ) or Veh (0.9% normal saline). At  $t = -90$  min, a continuous intravenous (i.v.) infusion of [ $3\text{-}^3\text{H}$ ] glucose was commenced (10  $\mu\text{Ci}$  bolus + 0.05  $\mu\text{Ci}\cdot\text{min}^{-1}$ ). Blood samples were taken at  $t = -10$  and 0 min to calculate the basal glucose turnover rate (GTR), which at steady state is equal to the rates of both glucose production and glucose disposal, and the peripheral glucose clearance rate (calculated as the glucose disposal rate divided by the plasma glucose concentration<sup>18</sup>).

### Frequently sampled intravenous glucose tolerance test (FSIGT)

Following the basal glucose turnover study, the same cohort of *ob/ob* (B6) mice was subjected to an FSIGT. Blood sampling was performed via an arterial catheter in unrestrained, conscious animals. A continuous infusion of saline-washed erythrocytes was commenced at  $t = 0$  min to prevent a  $>5\%$  fall in hematocrit. Baseline fasting blood samples were drawn at  $-10$  and  $0$  min. Based on a published protocol<sup>22</sup>, a bolus of 50% dextrose (0.75 g/kg body weight) was injected iv over a period of 15s at  $t = 0$  min. Blood (20  $\mu$ l) was sampled both for measurement of glucose using a hand-held glucometer (Accu-Chek Aviva Plus, Roche; Indianapolis, IN ) and for subsequent assay of plasma insulin and lactate levels at time points 1, 2, 4, 8, 12, 16, 20, 30 and 60 min after the glucose injection. Additional samples were obtained for blood glucose measurement at 3, 5, 6, 10, 14, 18, 25, 40 and 50 min using a hand-held glucometer.

### Minimal Model analysis and calculations

The plasma insulin and blood glucose profiles generated from the FSIGTs were analyzed using MinMod software to quantify insulin-independent glucose disposal ( $S_G$ ) and insulin sensitivity ( $S_I$ ), as previously described<sup>22</sup>. From the FSIGT, insulin secretion was quantified as the acute insulin response to glucose ( $AIR_g$ ), a measure of islet  $\beta$ -cell function in response to a glucose load, based on plasma insulin values between  $t = 0-4$  min<sup>22</sup>.

### 2-[<sup>14</sup>C] deoxyglucose ([2-<sup>14</sup>C]DG) study

7 d after *ob/ob* (C6) mice received i.c.v. injection via the LV of either mFGF1 (3  $\mu$ g) or Veh (0.9% normal saline), a 13  $\mu$ Ci dose of [2-<sup>14</sup>C]DG was administered via the jugular vein to assess tissue-specific glucose clearance ( $K_g$ ;  $\mu$ l/min/mg tissue). At  $t = 5, 15, 25$  and  $35$  min, arterial blood was sampled to measure blood glucose and [2-<sup>14</sup>C]DG. Subsequently, the mice were anesthetized and the following tissues were excised, immediately frozen in liquid nitrogen, and stored at  $-80$  °C until future tissue analysis: skeletal muscle [soleus, tibialis anterior, gastrocnemius and superficial white vastus lateralis], visceral epididymal white adipose tissue (EWAT), subcutaneous gonadal adipose tissue (SubQ WAT), brown adipose tissue (BAT), heart and brain.

### Plasma and tissue analysis

Blood samples were collected into EDTA-treated tubes for measurement of plasma hormones and metabolites. Whole blood was centrifuged and plasma removed for subsequent measurement of plasma immunoreactive insulin [either by ELISA (Crystal Chem, Inc., IL) or by a radioimmunoassay kit from Millipore (Billerica, MA; performed by the Vanderbilt Diabetes Center Hormone Assay & Analytical Services Core)], and for measurement of glucagon and corticosterone levels by ELISA (Mercodia, Winston Salem, NC; and ALPCO Diagnostics, Salem, NH). Plasma lactate levels were determined using a GM9D glucose direct analyzer (Analox Instruments, UK). Plasma lipids were measured with enzymatic colorimetric assays using the following kits: Triglycerides and total cholesterol from Raichem (San Diego, CA); non-esterified free fatty acid (NEFA) from Wako Diagnostics (Richmond, VA). Liver glycogen levels were determined using a colorimetric assay (Biovision, Milpitas, CA) and were normalized to grams wet weight. For

the basal glucose turnover and [2-<sup>14</sup>C]DG, radioactivity of [3-<sup>3</sup>H] glucose and [2-<sup>14</sup>C]DG were processed as previously described<sup>44</sup> and determined by scintillation counting.

## RT-PCR

Total RNA was extracted from hypothalamus, liver and BAT using TriReagent (Sigma-Aldrich, St Louis, MO) and NucleoSpin RNA (Fischer Scientific, Federal Way, WA). Levels of specific transcripts were quantified by real-time PCR (ABI Prism 7900 HT; Applied Biosystems, Foster City, CA) using SYBR Green (Applied Biosystems) and the following specific primers: *Gck* (forward-CAAGCTGCACCCGAGCTT; reverse-TGATTCGATGAAGGTGATTTCCG), *Pklr* (forward-TGATGATTGGACGCTGCAA; reverse-CATTGGCCACATCGCTTG), *Gys2* (forward-ACCAAGGCCAAAACGACAG; reverse-GGGCTCACATTGTTCTACTTGA), *Pck1* (forward-GGCGGAGCATATGCTGATCC; reverse-CCACAGGCACTAGGGAAGGC), *G6pc* (forward-TCAACCTCGTCTTCAAGTGGATT; reverse-CTGCTTTATTATAGGCACGGAGCT), *Ucp1* (forward-ACTGCCACACCTCCAGTCATT; reverse-CTTGCCTCACTCAGGATTGG) and *Hspb1* (forward-ACGCAACCACTTCGCTCCGGAGG; reverse-CTTGGCTCCAGACTGTTCCAGACTTCGCTGAC). Results were normalized to the housekeeping gene *Rn18s* (forward-CGGACAGGATTGACAGATTG; reverse-CAAATCGCTCCACCAACTAA) to correct for internal variances. For comparative analysis, RNA ratios of the treatment group were normalized to the i.c.v. Veh control group.

## Systemic administration of insulin receptor antagonist

DIO WT mice (fed a HFD for 3 mo), chow-fed LIRFKO and littermate IRF fl/fl control mice underwent LV cannulation. Following a 1 week recovery, mice underwent sc implantation of an osmotic micropump (Alzet, Durect Corp., Cupertino, CA) loaded with the high affinity insulin receptor antagonist S961 (dissolved in PBS; a generous gift from Novo Nordisk) at a dose designed to continuously infuse the drug at a rate of either 29 nmol/week for the HFD-fed or 25 nmol/week for the chow-fed mice for 2 week. On Day 2 or 3, following micropump implantation, the mice received a single i.c.v. injection of either mFGF1 (3 µg) or Veh (0.9% normal saline). Daily blood glucose levels, food intake and body weight were recorded throughout the study.

## Effect of i.c.v. FGF1 and FGF19 on c-Fos induction in hypothalamic tanycytes

To assess induction of c-fos in 3<sup>rd</sup> ventricular tanycytes in response to central administration of either FGF1 or FGF19, FGFR1-EGFP transgenic mice underwent LV cannulation. Following 1-week recovery, habituated animals were fasted for 5 h and then received an i.c.v. injection of Veh, mFGF1 (3 µg), or hFGF19 (3 µg). Ninety minutes later, mice were anesthetized with ketamine/xylazine, perfused with PBS followed by 4% paraformaldehyde (PFA) in 0.1M PBS, and brains removed and processed for immunohistochemical analysis. Briefly, sections were incubated in rabbit anti-c-Fos antibody (1:100,000; PC38; Oncogene Research Products, Boston, MA), followed by incubation in donkey anti-rabbit Alexa 594 (1:1,000; Molecular Probes, Inc., Eugene, OR). Although these studies were conducted in transgenic mice in which GFP expression is driven by the FGFR1 promoter, co-localization of GFP staining with c-Fos was not performed due to concerns regarding the extent to which

GFP expression is specific to FGFR1<sup>+</sup> cells in these mice. C-Fos was quantified from the cells (both ependymal and tanycytes) lining the 3<sup>rd</sup> ventricle from anatomically matched hypothalamic sections using Image J software (NIH).

### Effect of i.c.v. FGF1 on HSP25 expression in hypothalamic tanycytes and astrocytes

Adult, male WT mice were sacrificed 24 h after receiving i.c.v. injections via the LV of mFGF1 (3 µg) or Veh. After cervical dislocation, the brain was extracted and wholemounts of the 3<sup>rd</sup> ventricle walls, including the hypothalamus, were dissected and fixed in 4% PFA/0.1% Triton X-100 (TX) overnight at 4°C. Wholemounts were incubated in primary and secondary antibodies in PBS with 0.5% TX and 10% normal goat or donkey serum for 24 h at 4°C. Primary antibodies: rabbit anti-mouse HSP25 (homologous to human HSP27; 1:500; SPA801, Enzo Life Sciences, Farmingdale, NY), mouse anti-GFAP (1:10,000; C9205; Sigma Aldrich, St Louis, MO), and chicken anti-vimentin (1:1,000; EMD Millipore AB5733, Billerica, MA). Secondary antibodies: conjugated to Alexa Fluor dyes (1:1,000; goat or donkey polyclonal, Molecular Probes, Thermo Scientific, Rockford, IL). After staining, the ventricular walls were dissected from underlying parenchyma as slivers of tissue 300–400 µm thick and mounted on a slide with mounting media and a coverslip. Confocal images were taken on a Leica SP5 (Leica Microsystems Inc., Buffalo Grove, IL). Quantification of vimentin or GFAP co-expression in HSP25<sup>+</sup> cells was performed in 3 high-power confocal images (116.4 × 116.4 µm<sup>2</sup>) evenly spaced across the ventral to dorsal span of the HSP25<sup>+</sup> band in the posterior 3<sup>rd</sup> ventricle.

### Western blot

Brains were removed, hypothalami were dissected and quickly frozen on dry ice and stored at –80°C. Total protein lysates were prepared by homogenizing hypothalami in 3 volumes of lysis buffer (T-PER, Thermo Scientific, Rockford, IL) containing protease inhibitor cocktail (cOmplete; Sigma Aldrich, St Louis, MO) and phosphatase inhibitors (phosSTOP Phosphatase Inhibitor Cocktail Tablets; Roche, Indianapolis, IN). Homogenates were centrifuged and the supernatants retained for western analysis. Protein concentrations were determined with the BCA Protein Assay Kit (Pierce, Thermo Scientific, Rockford, IL). Proteins (40 µg/lane) were separated on a 10% precast SDS-PAGE gel (Invitrogen, Carlsbad, CA). After electrophoresis at 100V for 90 min, the proteins were transferred for 1 h at 4 °C onto nitrocellulose membranes (Millipore, Billerica, MA). The membranes were blocked in 5% non-fat milk for 1 h. Membranes were incubated overnight (at 4°C) with rabbit anti-synaptophysin (1:1,000; SAB4502906, Sigma Aldrich, St Louis, MO) or rabbit anti-β-Tubulin III (Tuj 1; 1:1,000, T3952, Sigma Aldrich, St Louis, MO). Following washes with tris-buffered saline, 0.05% Tween-20 (TBST), membranes were incubated 1 h with HRP-conjugated donkey anti-rabbit (1:5,000; Cell Signaling Technology, Danvers, MA) and visualized using the Pierce ECL kit (Thermo Scientific, Rockford, IL). Blots were scanned and quantified using Image J software (NIH). All protein band density was normalized to the loading control β-tubulin III.

### Statistical analysis

For each study, groups receiving i.c.v. Veh vs. FGF1 (or FGF19) were matched for age, body weight and blood glucose levels. Sample sizes of 6–8/group were predicated on detecting

with ~80% power a blood glucose group difference of 100 mg/dl assuming a within group standard deviation of 55 mg/dl. Group by time mixed factorial designs were analyzed using linear mixed model analysis (SPSS v. 23, IBM Corp., Somers, NY) and mixed factorial analyses (GraphPad software, La Jolla, CA). Basic pairwise comparisons were by independent samples t-tests with Satterthwaite adjustment for unequal variances where indicated by significant Levene's tests. Within time-point pairwise assessments of group differences were rendered in terms of 95% confidence intervals to convey effect sizes and their patterns over time. A two-sample unpaired Student's *t*-test was used for two-group comparisons and a one-way ANOVA was performed for three-group comparisons. Data met the normality assumptions of the statistical tests. Animals were not excluded from the studies unless otherwise indicated and the investigators were not blinded to study conditions. Alpha was set at  $P < 0.05$ , 2-tail.

## Supplementary Material

Refer to Web version on PubMed Central for supplementary material.

## Acknowledgments

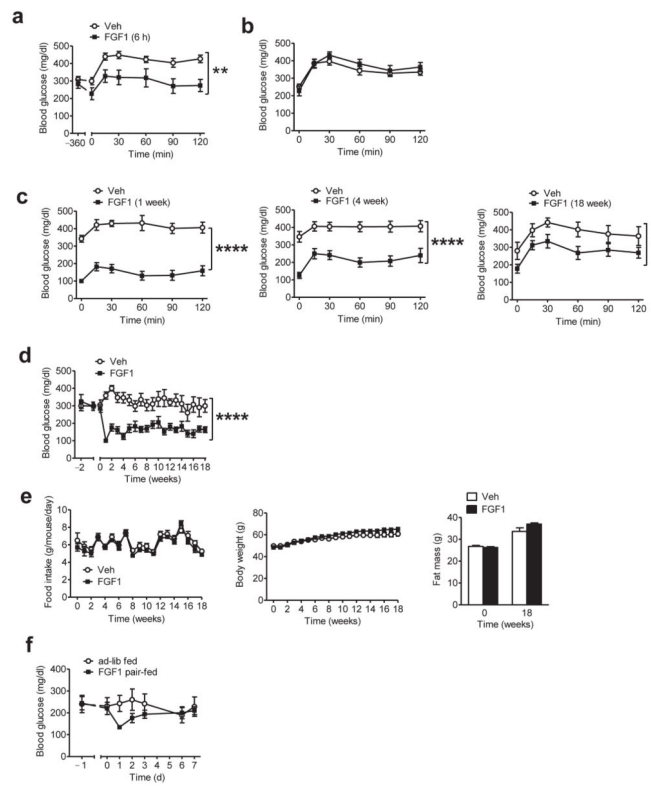
The authors are grateful to the Vanderbilt University Mouse Metabolic Phenotyping Center (DK059637) for the performance of the basal glucose turnover, FSIGT and [2-<sup>14</sup>C]DG studies, the Nutrition Obesity Research Center (DK035816), the Diabetes Research Center (DK017047) at the University of Washington, and the technical assistance provided by T. Meek, V. Damian, L. Nguyen, T. Harvey, and J. Brown at the University of Washington, and D. Bracy and A. Locke at Vanderbilt University. We gratefully acknowledge L. Schäffer (Novo Nordisk) for providing the insulin receptor antagonist (S961). This work was supported by research grants from the US National Institute of Diabetes and Digestive and Kidney Diseases Grant Nos. DK083042, DK090320, DK101997 (M.W.S.), DK089056 (G.J.M.), DK007742, DK104461 (J.M.S.), DK007247, DK103375 (J.M.R.), DK27619, DK29867 (R.N.B), the Department of Veterans Affairs Merit Review Program (T.G.U), and by funding supplied by Novo Nordisk (M.W.S).

## REFERENCES FOR MAIN TEXT

1. IDF Diabetes Atlas. International Diabetes Federation (IDF). 7. Brussels; Belgium: 2015.
2. Morton GJ, et al. FGF19 action in the brain induces insulin-independent glucose lowering. *The Journal of clinical investigation*. 2013; 123:4799–4808. [PubMed: 24084738]
3. Marcelin G, et al. Central action of FGF19 reduces hypothalamic AGRP/NPY neuron activity and improves glucose metabolism. *Molecular metabolism*. 2014; 3:19–28. [PubMed: 24567901]
4. Ryan KK, et al. Fibroblast growth factor-19 action in the brain reduces food intake and body weight and improves glucose tolerance in male rats. *Endocrinology*. 2013; 154:9–15. [PubMed: 23183168]
5. Ornitz DM, Itoh N. The Fibroblast Growth Factor signaling pathway. *Wiley interdisciplinary reviews Developmental biology*. 2015; 4:215–266. [PubMed: 25772309]
6. Schwartz MW, et al. Cooperation between brain and islet in glucose homeostasis and diabetes. *Nature*. 2013; 503:59–66. [PubMed: 24201279]
7. Grayson BE, Seeley RJ, Sandoval DA. Wired on sugar: the role of the CNS in the regulation of glucose homeostasis. *Nature reviews Neuroscience*. 2013; 14:24–37. [PubMed: 23232606]
8. Fu L, et al. Fibroblast growth factor 19 increases metabolic rate and reverses dietary and leptin-deficient diabetes. *Endocrinology*. 2004; 145:2594–2603. [PubMed: 14976145]
9. Xu J, et al. Acute glucose-lowering and insulin-sensitizing action of FGF21 in insulin-resistant mouse models--association with liver and adipose tissue effects. *Am J Physiol Endocrinol Metab*. 2009; 297:E1105–1114. [PubMed: 19706786]
10. Suh JM, et al. Endocrinization of FGF1 produces a neomorphic and potent insulin sensitizer. *Nature*. 2014; 513:436–439. [PubMed: 25043058]

11. Ito J, et al. Astrocytes produce and secrete FGF-1, which promotes the production of apoE-HDL in a manner of autocrine action. *Journal of lipid research*. 2005; 46:679–686. [PubMed: 15627653]
12. Oomura Y, et al. A new brain glucosensor and its physiological significance. *The American journal of clinical nutrition*. 1992; 55:278S–282S. [PubMed: 1370249]
13. Suzuki S, et al. Feeding suppression by fibroblast growth factor-1 is accompanied by selective induction of heat shock protein 27 in hypothalamic astrocytes. *The European journal of neuroscience*. 2001; 13:2299–2308. [PubMed: 11454034]
14. Lou G, et al. Intranasal administration of TAT-haFGF((1)(4)(-)(1)(5)(4)) attenuates disease progression in a mouse model of Alzheimer's disease. *Neuroscience*. 2012; 223:225–237. [PubMed: 22885230]
15. Cheng X, et al. Acidic fibroblast growth factor delivered intranasally induces neurogenesis and angiogenesis in rats after ischemic stroke. *Neurological research*. 2011; 33:675–680. [PubMed: 21756545]
16. Jonker JW, et al. A PPARgamma-FGF1 axis is required for adaptive adipose remodelling and metabolic homeostasis. *Nature*. 2012; 485:391–394. [PubMed: 22522926]
17. Perry RJ, et al. FGF1 and FGF19 reverse diabetes by suppression of the hypothalamic-pituitary-adrenal axis. *Nature communications*. 2015; 6:6980.
18. Best JD, Taborsky GJ Jr, Halter JB, Porte D Jr. Glucose disposal is not proportional to plasma glucose level in man. *Diabetes*. 1981; 30:847–850. [PubMed: 6115785]
19. Kahn SE, et al. The contribution of insulin-dependent and insulin-independent glucose uptake to intravenous glucose tolerance in healthy human subjects. *Diabetes*. 1994; 43:587–592. [PubMed: 8138065]
20. Gresl TA, et al. Dietary restriction and glucose regulation in aging rhesus monkeys: a follow-up report at 8.5 yr. *American journal of physiology Endocrinology and metabolism*. 2001; 281:E757–765. [PubMed: 11551852]
21. Ader M, Pacini G, Yang YJ, Bergman RN. Importance of glucose per se to intravenous glucose tolerance. Comparison of the minimal-model prediction with direct measurements. *Diabetes*. 1985; 34:1092–1103. [PubMed: 2864297]
22. Alonso LC, et al. Simultaneous measurement of insulin sensitivity, insulin secretion, and the disposition index in conscious unhandled mice. *Obesity (Silver Spring)*. 2012; 20:1403–1412. [PubMed: 22331130]
23. Rojas JM, et al. Glucose intolerance induced by blockade of central FGF receptors is linked to an acute stress response. *Molecular metabolism*. 2015; 4:561–568. [PubMed: 26266088]
24. Stefanovski D, et al. Estimating hepatic glucokinase activity using a simple model of lactate kinetics. *Diabetes care*. 2012; 35:1015–1020. [PubMed: 22456868]
25. Davis MA, Williams PE, Cherrington AD. Net hepatic lactate balance following mixed meal feeding in the four-day fasted conscious dog. *Metabolism*. 1987; 36:856–862. [PubMed: 3306279]
26. King AJ. The use of animal models in diabetes research. *British journal of pharmacology*. 2012; 166:877–894. [PubMed: 22352879]
27. Porte D Jr. Banting lecture 1990. Beta-cells in type II diabetes mellitus. *Diabetes*. 1991; 40:166–180. [PubMed: 1991568]
28. Schaffer L, et al. A novel high-affinity peptide antagonist to the insulin receptor. *Biochem Biophys Res Commun*. 2008; 376:380–383. [PubMed: 18782558]
29. Lu M, et al. Insulin regulates liver metabolism in vivo in the absence of hepatic Akt and Foxo1. *Nature medicine*. 2012; 18:388–395.
30. O-Sullivan I, et al. FoxO1 integrates direct and indirect effects of insulin on hepatic glucose production and glucose utilization. *Nature communications*. 2015; 6:7079.
31. Titchenell PM, Chu Q, Monks BR, Birnbaum MJ. Hepatic insulin signalling is dispensable for suppression of glucose output by insulin in vivo. *Nature communications*. 2015; 6:7078.
32. Orellana JA, et al. Glucose increases intracellular free Ca<sup>2+</sup> in tanycytes via ATP released through connexin 43 hemichannels. *Glia*. 2012; 60:53–68. [PubMed: 21987367]
33. Robins SC, et al. alpha-Tanycytes of the adult hypothalamic third ventricle include distinct populations of FGF-responsive neural progenitors. *Nature communications*. 2013; 4:2049.

34. Stetler RA, Gao Y, Signore AP, Cao G, Chen J. HSP27: mechanisms of cellular protection against neuronal injury. *Current molecular medicine*. 2009; 9:863–872. [PubMed: 19860665]
35. Mirzadeh Z, Doetsch F, Sawamoto K, Wichterle H, Alvarez-Buylla A. The subventricular zone en-face: wholemount staining and ependymal flow. *Journal of visualized experiments : JoVE*. 2010
36. Fischer A, Sananbenesi F, Wang X, Dobbin M, Tsai LH. Recovery of learning and memory is associated with chromatin remodelling. *Nature*. 2007; 447:178–182. [PubMed: 17468743]
37. Pinto JG, Jones DG, Williams CK, Murphy KM. Characterizing synaptic protein development in human visual cortex enables alignment of synaptic age with rat visual cortex. *Frontiers in neural circuits*. 2015; 9:3. [PubMed: 25729353]
38. Moore MC, Coate KC, Winnick JJ, An Z, Cherrington AD. Regulation of hepatic glucose uptake and storage in vivo. *Adv Nutr*. 2012; 3:286–294. [PubMed: 22585902]
39. Elizondo-Vega R, et al. The role of tanycytes in hypothalamic glucosensing. *Journal of cellular and molecular medicine*. 2015; 19:1471–1482. [PubMed: 26081217]
40. Bolborea M, Dale N. Hypothalamic tanycytes: potential roles in the control of feeding and energy balance. *Trends in neurosciences*. 2013; 36:91–100. [PubMed: 23332797]
41. Paxinos, G.; Watson, C. *The Rat Brain in Stereotaxic Coordinates*. Academic Press; San Diego: 1998.
42. Franklin, KBJ.; Paxinos, G. *The Mouse Brain in Stereotaxic Coordinates*. Academic Press; San Diego: 1997.
43. Ayala JE, Bracy DP, McGuinness OP, Wasserman DH. Considerations in the design of hyperinsulinemic-euglycemic clamps in the conscious mouse. *Diabetes*. 2006; 55:390–397. [PubMed: 16443772]
44. Otero YF, et al. Enhanced Glucose Transport, but not Phosphorylation Capacity, Ameliorates Lipopolysaccharide-Induced Impairments in Insulin Stimulated-Muscle Glucose Uptake. *Shock*. 2015

**FIGURE 1.**

Diabetes remission induced by a single i.c.v. FGF1 injection in *ob/ob* mice. **(a,b)** Blood glucose levels during an intraperitoneal glucose tolerance test (ipGTT) performed in fasted *ob/ob* (B6) mice 6 h after **(a)** a single i.c.v. injection of either vehicle (Veh; open symbols;  $n = 8$ ) or 3  $\mu\text{g}$  of mFGF1 (black symbols;  $n = 9$ ), or **(b)** a single s.c. injection of either Veh or the same dose of mFGF1 (Veh,  $n = 7$ ; FGF1,  $n = 6$ ). **(c)** Blood glucose values from an ipGTT performed in fasted *ob/ob* (B6) mice either 7 d (left), 4 weeks (middle), or 18 weeks (right) following a single i.c.v. injection of mFGF1 (3  $\mu\text{g}$ ). **(d)** Time course of blood glucose levels from the same cohort of *ad-libitum* (*ad-lib*)-fed *ob/ob* mice both prior to and after a single i.c.v. injection of mFGF1 (3  $\mu\text{g}$ ). **(e)** Food intake (left), body weight (middle), and fat mass (right) of *ob/ob* (B6) mice following i.c.v. injection of either mFGF1 or Veh. **(f)** Daily blood glucose levels from i.c.v. Veh-injected *ob/ob* mice that were fed either *ad-lib* ( $n = 10$ ) or pair-fed to a separate cohort of mice that had received i.c.v. mFGF1 (3  $\mu\text{g}$ ;  $n = 10$ ). Data are the mean  $\pm$  s.e.m. \* $P < 0.05$ , \*\* $P < 0.01$ , \*\*\*\* $P < 0.0001$  for group (Veh vs. FGF1) by repeated measures designs by linear mixed model analyses.

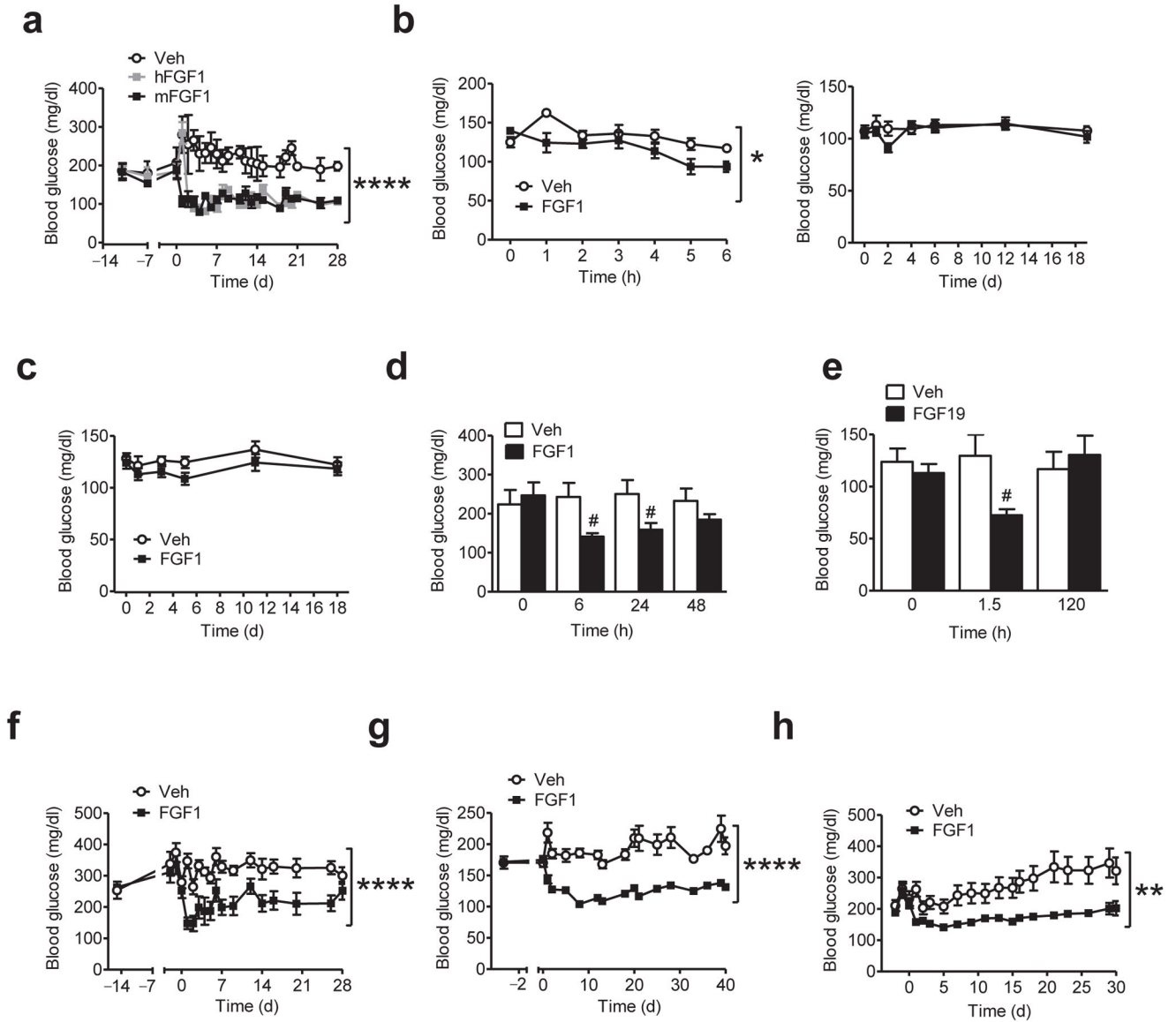


**FIGURE 2.**

Diabetes remission induced by a single i.c.v. FGF1 injection across multiple rodent models of T2D. **(a)** Daily blood glucose levels from *ad-lib-fed ob/ob* (B6) mice following a single i.c.v. injection of either hFGF1 (3  $\mu$ g;  $n$  = 6; grey symbols), mFGF1 (3  $\mu$ g;  $n$  = 6; black symbols), or Veh ( $n$  = 4; open symbols). **(b)** Fasting blood glucose values (left) from lean, wild-type (WT) mice 6 h after i.c.v. injection of either mFGF1 (3  $\mu$ g;  $n$  = 5) or Veh ( $n$  = 5), and daily blood glucose levels (right) from WT mice *ad-lib-fed* (standard chow) following a single i.c.v. injection of mFGF1 (3  $\mu$ g;  $n$  = 8), or Veh ( $n$  = 8). **(c)** Daily blood glucose levels from WT *ad-lib-fed* DIO mice following a single i.c.v. injection of mFGF1 (3  $\mu$ g;  $n$  = 8), or Veh ( $n$  = 8). **(d)** Blood glucose values from *ad-lib-fed ob/ob* (B6) mice following a single s.c. injection of either mFGF1 (0.5 mg/kg body weight;  $n$  = 11) or Veh ( $n$  = 10). **(e)** Fasting (before and 1.5 h after i.c.v. injection) and *ad-lib-fed* blood glucose levels (120 h) from *ob/ob* (B6) mice receiving i.c.v. injection of either FGF19 (3  $\mu$ g;  $n$  = 5) or Veh ( $n$  = 5). **(f)**

Time course of blood glucose levels from *ad-lib*-fed *db/db* mice both prior to and following a single i.c.v. injection of mFGF1 (3  $\mu$ g;  $n = 6$ ) or Veh ( $n = 9$ ). (g) Time course of blood glucose levels from *ad-lib*-fed DIO WT mice rendered diabetic with a low dose of STZ (DIO-LD STZ) both prior to and following a single i.c.v. injection of mFGF1 (3  $\mu$ g;  $n = 8$ ) or Veh ( $n = 8$ ). (h) Daily blood glucose levels from *ad-lib*-fed ZDF rats following a single i.c.v. injection of either rFGF1 (3  $\mu$ g;  $n = 10$ ; black symbols) or Veh ( $n = 10$ ; open symbols). Data are the mean  $\pm$  s.e.m. \* $P < 0.05$ , \*\* $P < 0.01$ , \*\*\*\* $P < 0.0001$  for group (Veh vs. FGF1) by repeated measures designs by linear mixed model analyses. # $P < 0.05$ , FGF1 (or FGF19) vs. Veh as determined by two-tailed t-test.

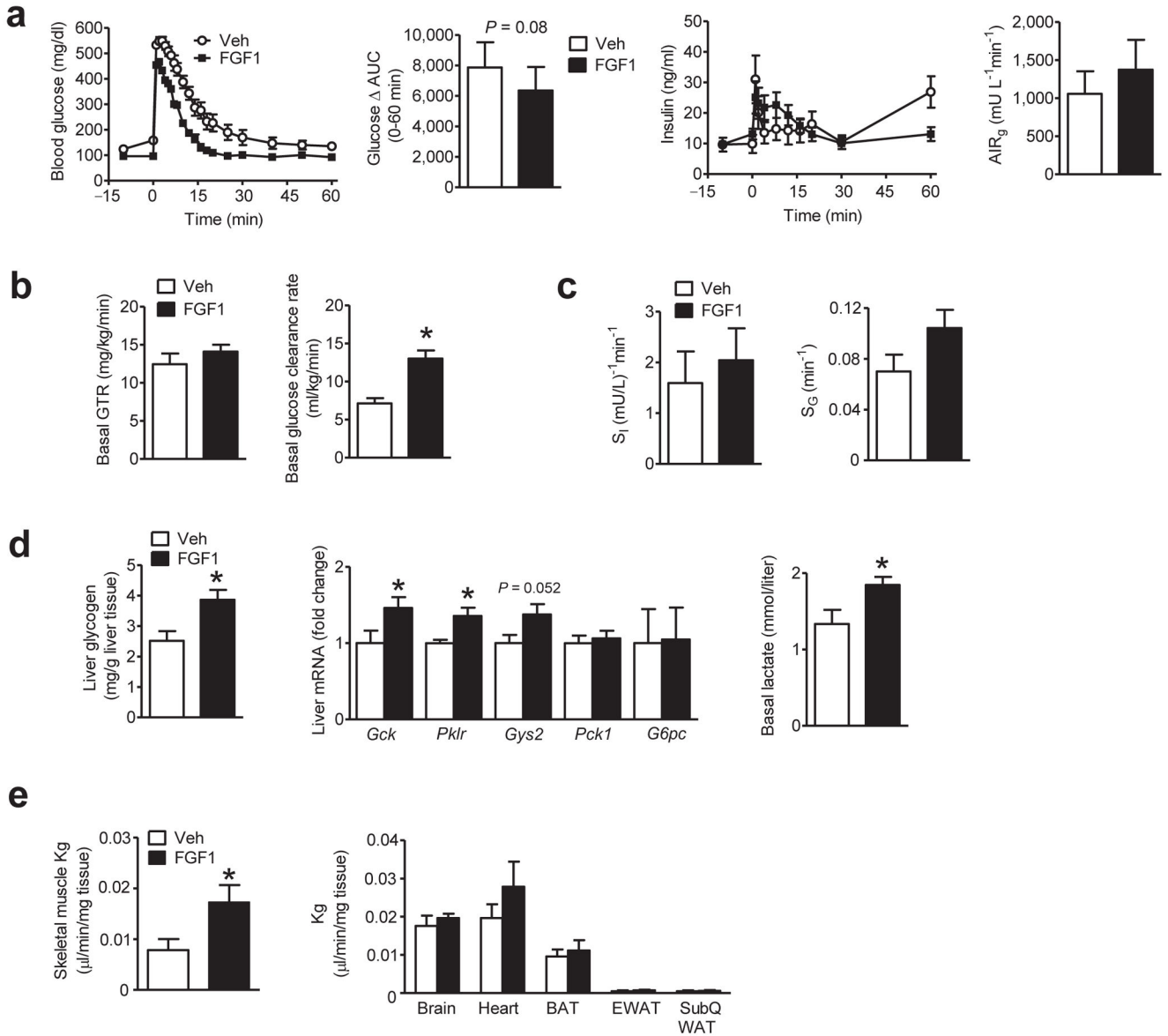


**FIGURE 3.**

Effect a single i.c.v. injection of FGF1 on whole-body glucose kinetics in *ob/ob* mice. *ob/ob* (B6) mice underwent a basal glucose turnover study followed by a frequently sampled intravenous glucose tolerance test (FSIGT) 7 d after a single i.c.v. injection of mFGF1 (3  $\mu$ g, black symbols;  $n = 13$ ) or Veh (open symbols;  $n = 9$ ). **(a)** Fasting blood glucose levels (left), and delta area under the glucose curve ( $\Delta$  AUC) during the FSIGT (after correcting for differences of basal glucose; middle); plasma insulin levels (middle), and the acute insulin response to glucose (AIR<sub>g</sub>) during the FSIGT (right). **(b)** Mean basal glucose turnover rate (GTR; left) and basal glucose clearance rate (right). **(c)** Insulin sensitivity (S<sub>I</sub>; left), insulin-independent glucose disposal (S<sub>G</sub>; right) **(d)** Liver glycogen content (left) and levels of mRNA encoding liver gluco regulatory genes from samples obtained at study termination (middle); basal plasma lactate levels obtained prior to the FSIGT (right). **(e)** Glucose

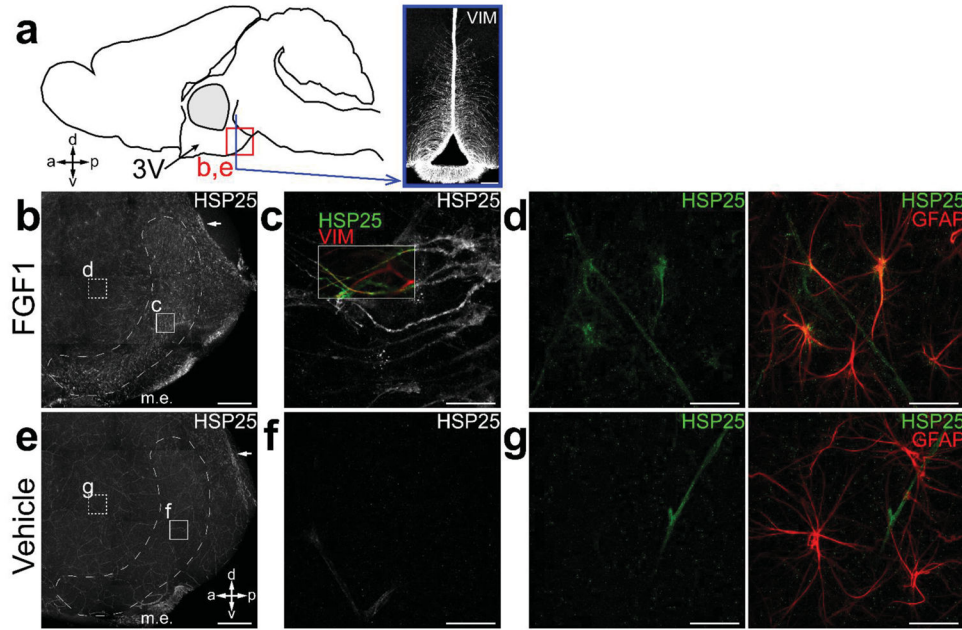
clearance rate ( $K_g$ ) determined from steady-state iv infusion of  $[2-^{14}C]DG$  in tissues including skeletal muscle (left), and brain, heart, BAT, EWAT and s.c. WAT (right) in *ob/ob* mice 7 d after a single i.c.v. injection of mFGF1 (3  $\mu g$ ,  $n = 7$ ) or Veh ( $n = 6$ ). Data are mean  $\pm$  s.e.m. \* $P < 0.05$ , FGF1 vs. Veh as determined by two-tailed t-test. n.s., non-significant.

Author Manuscript

Author Manuscript

Author Manuscript

Author Manuscript

**FIGURE 4.**

HSP25 expression in whole-mounts of the 3rd ventricle wall in response to i.c.v. FGF1. (a) Diagram illustrating the en-face whole-mount perspective and the relative location of the posterior ventral 3rd ventricle in a mid-sagittal view of the mouse brain. The square outlines the region imaged in (b) and (e). (b,e) Representative images of confocal z-stacks (b; of  $n = 4$  images, c; of  $n = 4$  images) spanning  $80\ \mu\text{m}$  from the ependymal surface deep into the parenchyma of posterior ventral 3rd ventricle from i.c.v. mFGF1- ( $3\ \mu\text{g}$ ) (b;  $n = 6$ ) and i.c.v. Veh-treated (e;  $n = 4$ ) WT mice. Inset letters show regions where the corresponding high power images were taken. Arrows point to a small subset of multi-ciliated ependymal cells seen in FGF1- and Veh-treated animals. m.e., median eminence. (c,f) Representative images of confocal z-stacks (c; of  $n = 30$  images, f; of  $n = 12$  images) of ventricular surface of 3rd ventricle showing HSP25 expression specifically following i.c.v. mFGF1 in vimentin (+) cells with elongated morphology, corresponding to tanycytes. (d,g) Representative images of confocal z-stacks (d; of  $n = 33$  images, g; of  $n = 12$  images) taken within the subependymal zone, showing HSP25 expression in stellate-shaped GFAP<sup>+</sup> astrocytes specifically following i.c.v. mFGF1. Scale,  $100\ \mu\text{m}$  (a),  $0.25\ \text{mm}$  (b,e), and  $10\ \mu\text{m}$  (c,d,f,g).